Electronic Structure of the Novel Phase-Change Material $GeCu_2Te_3$

K. Kobayashi and M. Kobata,
Quantum Beam Science Directory, Japan Atomic Energy Agency
Kouto 1-1-1, Sayo-cho, Sayo-gun, Hyogo Japan
Koba_kei@spring8.or.jp

J. Skelton and S. Elliott,
Department of Chemistry, University of Cambridge, Cambridge, CB2 1EW, UK.

Y. Saito, Y. Sutou, and J. Koike
Department of Materials Science, Graduate School of Engineering, Tohoku University,
6-6-11 Aoba-yama, Sendai 980-8579, Japan.

Key words: Phase Change, $GeCu_2Te_3$, HXPES, *Ab initio* molecular-dynamics simulation.

ABSTRACT

$GeCu_2Te_3$ (GCT) has been demonstrated as a potential phase-change material (PCM) for next-generation non-volatile memories by Sutou et al.[1-3] The phase transition takes place to a tetrahedrally-bonded crystal, a very different geometry to the octahedrally-bonded cubic structures of the conventional phase-change materials of $GeTe$-Sb_2Te_3 (GST) pseudo-binary alloys and related compounds. GCT was found to show a higher density and higher optical reflectivity in the amorphous phase than in the crystalline phase, also in contrast to the conventional PCMs. An electronic and chemical structure study of the amorphous and crystalline phases of GCT has been carried out by bulk-sensitive hard X-ray photoelectron spectroscopy (XPS) using a laboratory XPS system with monochromatic Cr Kα (5.4 keV) excitation. The results are compared with a computer-simulational study of CGT, which has been conducted very recently by the Cambridge University group. The simulation has been successful in giving consistent results in respect of the atomic-level structure and physical properties. The results also lead to hypotheses to account for the higher amorphous-phase density and optical reflectivity. Regarding a comparison with the HXPES results, the dominant features of the experimental valence-band spectra are well reproduced using the calculated partial density of states, except near the Fermi-level region. The simulation also shows the existence of two charge states of Ge atoms in the unit cell, consistent with the observed splitting of the Ge $2p_{3/2}$ spectra into two dominant components.

Introduction

As a novel PCM, the ternary alloy $GeCu_2Te_3$ (GCT) has been shown to have much promise by Sutou and his coworkers[1-3]. They have shown that GCT possesses better data-retention properties and reduced amorphisation power requirements, together with a relatively short crystallization time compared to GST $(GeTe)_x(Sb_2Te_3)_{1-x}$ [3]. The density of amorphous GCT (aGCT) is *greater* than the crystalline form (cGCT), and a volume change of +2–4% between the phases compares favorably to the -6.5% reported for GST films. This anomalous density behavior is expected to improve device cycling endurance [2,3]. Furthermore, it has recently been shown that GCT, in combination with other PCMs, can be used to form layered multi-bit devices that can be switched between any of their resistance levels in a single write operation [4].

One of the most interesting features of GCT that it has 24 s-p electrons per molecule (4 s-p electrons per atom on average). Actually, it was verified that cGCT adopts a "chalcopyrite-like" structure with 4-fold sp^3-like bonding in the crystalline phase. This fact means that GCT is a different family of PCM from that of GST and related compounds, where the average valence electron numbers are approximately 5. Thus, a resonance-bonding picture, which is considered to be effective in the GST family [5], is not applicable to an understanding of the PC mechanism in GCT.

In order to elucidate the PC mechanism and the origins of the above-mentioned anomalous properties, hard X-ray photoelectron spectroscopy (HXPES) investigations of the as-grown and annealed GCT films have been conducted using a laboratory HXPES system with Cr Kα (5.4 keV) excitation [6,7] by K. K and M. K at SPring-8. DFT-based theoretical calculations to elucidate the relation between the atomic structure and electronic and optical properties of both phases have also been conducted by J. S and S. E at Cambridge University [8].

In this paper, we present experimental and theoretical results to discuss the electronic structure and chemical bonding of cGCT and aGCT.

Methods

Stoichiometric, Ge-rich, and Cu-rich GCT films were deposited at Tohoku University by co-sputtering using GeTe, and CuTe targets onto Si substrates covered with 20 nm of SiO_2. The compositions of the films were controlled by the microwave-power ratio for the two targets, and were determined by ICP and SEM-EDX measurements. The electric resistance of the films was measured in the course of the annealing process in order to see the phase changes from as-deposited amorphous to crystalline phases, which accompany a sharp drop of the resistance. Crystalline structures were determined by XRD measurements, and optical-reflectance measurements were performed in a wavelength region between 250 and 1000 nm.

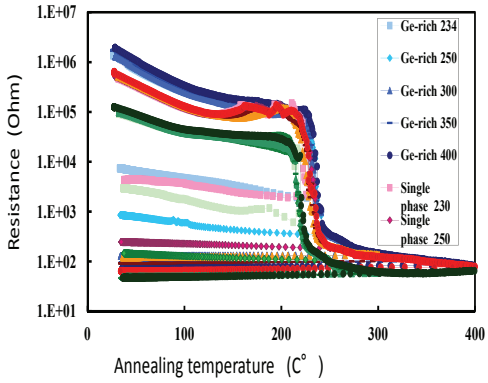

Fig. 1 Resistance vs. annealing temperature for GCT films.

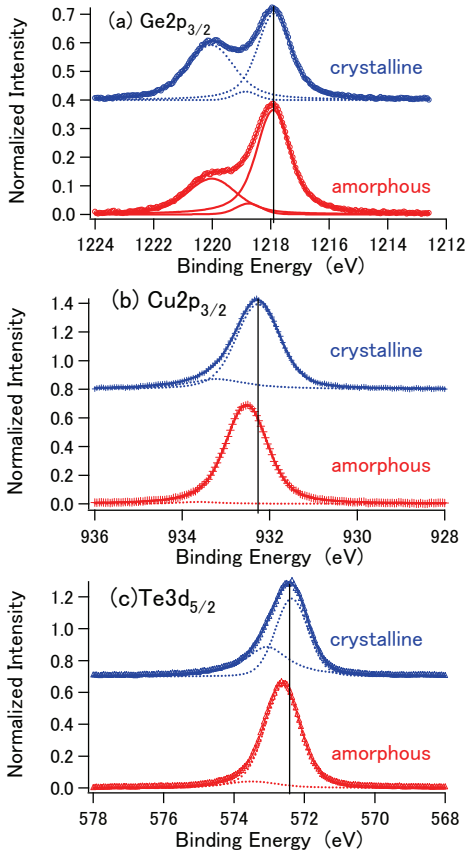

Fig. 2 $Ge2p_{3/2}$, $Cu2p_{3/}2$, and $Te3d_{5/2}$ spectra of cGCT and aGCT.

For HXPES measurements, samples were capped by C layers of a few nm soon after the GCT film deposition by sputtering. HXPES measurements were done using a laboratory system, with Cr Kα (5.4 keV) monochromatized X-rays for excitation (HEARP Lab) with an energy resolution of 0.55 eV [6,7]. The information depth is estimated to be ca. 10 nm. Thus, surface-oxidation-free spectra of the GCT films were able to be observed through the C capping layer. Valence-band Ge $2p_{3/2}$. Cu $2p_{3/2}$, and Te $3d_{5/2}$ spectra were measured. The Fermi edge of an Au plate was measured as an energy reference.

Ab initio molecular-dynamics (AIMD) simulations were carried out using the VASP code. A 96-atom model of cGCT, with a composition $Ge_{16}Cu_{32}Te_{48}$, was created by tiling the unit cell reported in [10], and the atomic positions were energy-relaxed within the fixed-size simulation cell. Models of aGcT were generated via an MD melt-quench procedure previously used with $Ge_2Sb_2Te_5$ [9]. Initial configurations in cubic supercells containing 96, 144, and 192 atoms, at the experimental crystalline density of 6.13 g cm^{-3} [10], were randomised by heating at 3000 K for 20 ps. Following this, the models were maintained in liquid states at 1200 K for 40 ps, before being quenched to 300K at a rate of -15 K ps^{-1}, which invariably led to amorphisation. The PBE functional [11], with PAW pseudopotentials, was used [12,13], including the semi-core Cu 3p and Ge 3d electrons. Spin-polarized calculations were performed to ensure that any unpaired electrons on the Cu atoms would be treated correctly.

Results and Discussion

As shown in Fig. 1, the electric resistance of the as-deposited films steeply decreases in a narrow temperature region between 210 C° and 240 C°, due to crystallization. The Cu-rich films and Ge-rich films show lower and higher phase-change temperatures compared to the stoichiometric films, respectively. The resistivity values at room temperature before and after annealing are higher in Ge-rich films and lower in Cu-rich films, and those of the stoichiometric films are in-between. In the following, we mainly discuss the HXPES and theoretical calculation results on stoichiometric films.

In Fig. 2 (a), Ge $2p_{3/2}$, (b) Te $3d_{5/2}$, and (c) Cu $2p_{3/2}$ core-level spectra of stoichiometric cGCT and aGCT films are shown. Open circles are experimental data points. Curve fit results using Voigt functions are shown by solid (total) and dotted curves (components) for each spectrum. The Ge $2p_{3/2}$ spectrum consists of two dominant components with a trivial third component in-between. The high binding-energy component is slightly weaker, whereas the low binding- energy component is stronger in the amorphous phase (aGCT) compared to the crystalline phase (cGCT). The Te $3d_{5/2}$ spectrum of cGCT also shows two component features, with a higher intensity in the lower binding-energy component with an intensity ratio of

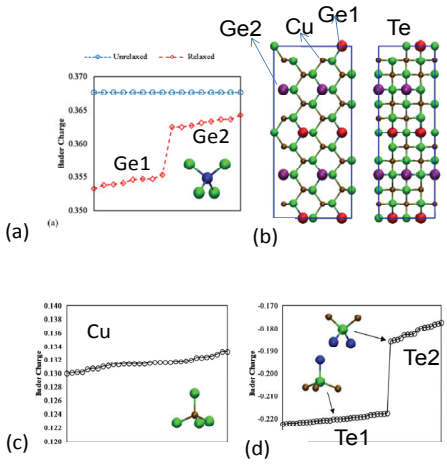

Fig. 3 Bader charge of (a)Ge, (c)Cu, and (d)Te., and (b) site distribution of two different Ge charge states in unit cell.

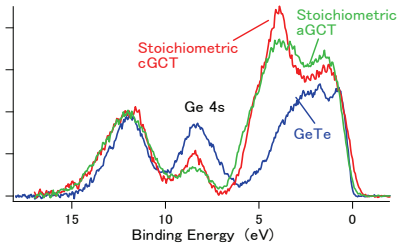

Fig. 4 Valence band spectra of cGCT, aGCT, and GeTe

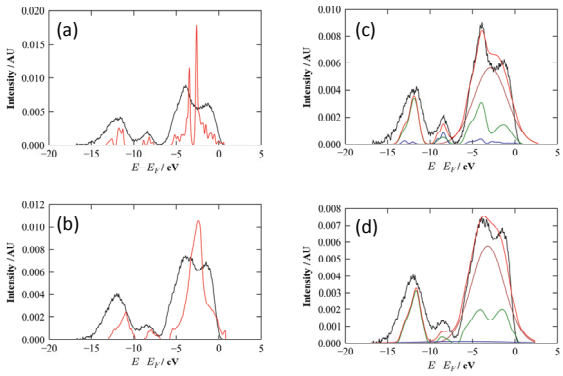

Fig. 5 Comparison between calculated DOS and experimental valence bans spectra of (a) cGCT and (b) aGCT. Curve fit results of valence band spectra using PDOSs introducing broadening and peak shifts for (b) cGCT and (d) aGCT.

1.85:1. The Cu $2p_{3/2}$ spectrum essentially consists of a single component, although an asymmetry in the lineshape increases slightly in the cGCT film compared to that of the aGCT fim.

There are two Te environments in cGCT, that is, the Te-centered tetrahedra $TeGeCu_3$and $TeGe_2Cu_2$. The population ratio of the two types of tetrahedra is 2:1. Thus, the two-component feature of the Te $3d_{5/2}$ spectrum in cGCT is naturally understood due to the differences in the Te environment. Actually, the observed intensity ratio is estimated as 1.85:1.1, very close to the expected ratio. However, the appearance of the dominant two components in the Ge $2p_{3/2}$ spectrum in cGCT is unexpected.

Fig. 3 shows calculated Bader charges of Ge, Te and Cu atoms in the model of cGCT. It is very striking that, while all sixteen Ge atoms have the same (positive) charge in the unrelaxed crystal model, energy relaxation reduces the average charge and causes the charges to split equally into two groups (Figure 3a). The two types of Ge atom undergo small displacements from their ideal crystallographic sites in a very similar manner to a Peierls transition, and the distortion lowers the energy by 90 meV/atom. The unit cell contains one of each type of Ge atom, which in the bulk system form layered arrangements coincident with the crystallographic axes of the unit cell, as schematically shown in Figure 3b. It should be noted that this charge splitting was only observed when a “hard” pseudopotential including the Ge 3d electrons was used, suggesting that it is related to a variation in the Ge core electronic configuration.

No similar splitting of the Cu or Te charges was observed on relaxation. The Cu atoms have a lower positive charge than that of either type of Ge, and the Te charges form two groups, corresponding to the two Te environments, with the $TeCu_3Ge$ sites having a more negative charge than $TeCu_2Ge_2$ sites, consistent with the experimentally observed splitting of the Te $3d_{5/2}$ spectra mentioned above.

Fig. 4 shows valence-band spectra of as-deposited (aGCT) and 350 C° annealed (cGCT) films. A valence-band spectrum of crystalline GeTe is also shown as a reference. Three dominant bands, that is, Te 5s at around 12 eV, Ge 4s band at around 8 eV, and the topmost band in the range 0-7 eV, of which dominant contributions come from Cu 3d and Te 5p states, are clearly resolved. Comparing with the GeTe spectrum, the Cu 3d contribution is recognizable at around 4 eV. The relative intensity of the Ge 4s band to the Te 5s band is weaker in GCT, due to the smaller relative Ge concentration. Considerable broadening is distinguishable in aGCT compared to cGCT. This is considered to be due to increased disorder in the a-phase.

The cGCT and aGCT spectra are compared with the calculated DOSs in Fig. 5(a) and (b). Sharp doublet peaks are manifest with broad tails towards higher and lower binding energies. The higher binding-energy sharp peak with the tail corresponds to Te 5s-Cu 3d bonding states. The tail towards lower binding energy is assigned to Te 5s-Cu 3d antibonding states. The sharp peak in between is the nonbonding state of Cu 3d, which inevitably appears due to an orientational mismatch of the Cu 3d orbitals relative to the tetrahedral sp^3 bonds of Te atoms. The experimental spectra show a much broader shape and the peak positions of these Cu 3d-Te 5s related states do not well coincide. The disagreements of the peak positions are mainly due to the effect of the final holes in a narrow band, in which the final hole is strongly localized; thus, the outgoing photoelectrons are strongly affected by the Coulomb attraction, giving a deeper binding energy in the observation than the calculated DOS. We corrected the positions of each peak in the partial density of states to get a better coincidence, as shown in Fig.5 (c) and (d) for cGCT and aGCT, respectively. We also introduced broadening to each PDOS in this fitting procedure. The Cu 3d band shows strong broadening, which suggests that the local disorder around the Cu atoms is appreciable.

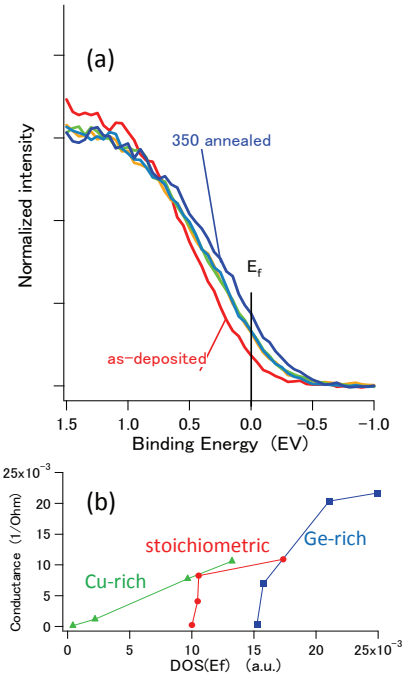

Fig. 6 (a) valence band spectra near Fermi level. (b) Conductance vs DOS(Ef)

The atomic-level structural calculation on aGCT in the same framework revealed a sharp peak at around 60° appearing in the Cu bond-angle distribution curve, indicating the presence of unusual threefold ring configurations. The calculated coordination numbers suggest that Ge and Te are fourfold-coordinated. Cu has a rather higher 6/7-fold coordination, around 35% of which, on average, comprises other Cu atoms. The experimentally observed higher density of aGCT [2] was reproduced in the simulations. The high density of aGCT may be related to the short Cu bonds observed in the simulations. The tetrahedral coordination in cGCT forces an "open" structure in which the lengths of Cu-Te and Ge-Te bonds must be accommodated. Shorter Cu bonding can occur in aGCT, allowing compact structural units, such as threefold rings, to form and leading to a higher density.

The optical reflectance was calculated through the dielectric function. The results well reproduced the experimental results in which the reflectance is higher in aGCT than in cGCT in the range from 250 nm to 1000 nm.

There is a disagreement in the DOS behavior near Fermi level. Fig. 6(a) shows the annealing temperature dependences of the valence-band spectral shape near the Fermi level of stoichiometric films. It is notable that the density of states, DOS(E_f), in a narrow region around the Fermi level increases as the annealing temperature increases. This is not reproduced in the theoretical calculations, as seen in Fig. 5(a) and (b), in which DOS(E_f) in the amorphous film is larger thanin the crystalline film.

Finally, we plotted the conductance at room temperature (C_a) for Cu-rich, stoichiometric, and Ge-rich annealed films as functions of DOS(E_f), as shown in Fig. 6(b). In Cu-rich films, C_a is proportional to DOS(E_f), suggesting that the mobility is annealing-temperature independent. In the stoichiometric and Ge-rich films, clear mobility edges are recognized. This result may be related to the differences in the local disorder in these films.

Conclusions

HXPES experiments and *ab initio* calculations have been conducted to elucidate electronic structure and chemical bonding states of the novel tetrahedrally bonded PC material, $GeCu_2Te_3$ (GCT). The results show that Ge atoms take two different charge states in the crystalline phase, in a manner reminiscent of a Peierls transition. The whole valence-band spectral shapes of cGCT and aGCT are well reproduced by calculated PDOSs when correcting the peak-position shift due to final–hole effects. The *ab initio* calculation gives a higher density of states at the Fermi level in aGCT than in cGCT. This disagrees with the experimental results, in which the spectral weight of aGCT at the Fermi level is less than that in cGCT. Plotting the electric conductance after annealing as functions of the density of states at the Fermi level determined by HXPES measurements revealed a mobility gap in stoichiometric and Ge-rich GCT films, whereas no gap is observed in Cu-rich films. In order fully to understand the PC phenomenon in materials with tetrahedral bonding, further investigations are needed.

References

[1] Y. Sutou, T. Kamada, M. Sumiya, Y. Saito, and J. Koike, Acta Mater. 60(3), 872 (2012).
[2] T. Kamada, Y. Sutou, M. Sumiya, Y. Saito, and J. Koike, Thin Solid Films 520(13), 4389 (2012).
[3] Y. Saito, Y. Sutou, and J. Koike, Appl. Phys. Lett. 102, 051910 (2013).
[4] Y. Saito, Y. H. Song, J. M. Lee, Y. Sutou, and J. Koike, IEEE Electron Device Lett. 33(10), 1399 (2012).
[5] M. Wuttig and N. Yamada, Nature Mater. 6(11), 824 (2007).
[6] M. Kobata, et al., Analytical Sci. 26, 1 (2010).
[7] K. Kobayashi, M. Kobata, and H. Iwai, J. Eelectron Spectroscopy and related Phenomena, HAXPES special issue, in print (available on line, http://www.sciencedirect.com/science/article/pii/S0368204813000704).
[8] J. Skelton, K. Kobayashi, Y. Sutou, and S. Elliott, Appl. Phys. Lett. **102**, 224105 (2013).
[9] J. M. Skelton, T. H. Lee, and S. R. Elliott, Appl. Phys. Lett. 101(2), 024106 (2012).
[10] G. E. Delgado, A. J. Mora, M. Pirela, A. Velasquez-Velasquez, M.Villarreal, and B. J. Fernandez, Phys. Status Solidi A 201(13), 2900 (2004).
[11] J. P. Perdew, K. Burke, and M. Ernzerhof, Phys. Rev. Lett. 77(18), 3865 (1996).
[12] P. E. Blochl, Phys. Rev. B 50(24), 17953 (1994).
[13] G. Kresse and D. Joubert, Phys. Rev. B 59(3), 1758 (1999).